Type of the Paper (Article)

Optical and Chromaticity Properties of Metal-Dielectric Composite-Based Multilayer Thin-Film Structures Prepared by RF Magnetron Sputtering

Mohammad Nur-E-Alam*, Md Momtazur Rahman, Mohammad Khairul Basher, Mikhail Vasiliev and Kamal Alameh

Electron Science Research Institute, School of Science, Edith Cowan University, 270 Joondalup Drive, Joondalup, WA, 6027, Australia; E-mail: m.nur-e-alam@ecu.edu.au (M. N.-E-A.), md.momtazur.rahman@outlook.com (M. M. R.), mkbasher@our.ecu.edu.au (M. K. B.), m.vasiliev@ecu.edu.au (M. V.) and k.alameh@ecu.edu.au (K. A.)

* Correspondence: m.nur-e-alam@ecu.edu.au;

Abstract: Over the last decades, the coated glass products, and especially the low-emissivity coatings have become a common building material used in modern architectural projects. More recently, these material systems became common in specialized glazing systems featuring solar energy harvesting. Apart from achieving the stability of optical parameters in multilayer coatings, it is also important to have improved control over the design of visual color properties of the coated glass. We prepare metal-dielectric composite (MDC) based multilayer thin-film structures using the RF-magnetron sputtering deposition and report on their optical and chromaticity properties in comparison with these obtained using pure metal-based Dielectric/Metal/Dielectric (DMD) trilayer structures of similar compositions. Experimentally achieved Hunter *L, a, b* values of MDC-based multilayer building blocks of coatings provide a new outlook on the engineering of future-generation optical coatings with better color consistency and developing approaches to broaden the range of achievable color coordinates and better environmental stability.

Keywords: metal-dielectric composites; multilayers; optical coatings; optical properties; color chromaticity; environmental stability.

1. Introduction

The prime cause of global warming is the continued use of fossil fuels. The excessive use of fossil fuels could lead to the non-renewable energy reserves being depleted, and that demands exploring novel materials and alternative technologies to minimise energy consumption. Besides the traditional industrial ways of "green" energy harvesting, the development of energy-efficient-buildings, building-integrated photovoltaic (BIPV) systems, and window coatings can represent the most sustainable approach to building a pathway towards a fossil-fuel-independent future and decreasing the CO_2 footprint [1-5]. Modern integrated PV technologies consisting of specialised thin-film coated glass, known as low-emissivity (Low-E) coatings, can cut either the heating-related, or the cooling-related (or in some cases, both) electric energy usage in buildings. The Low-E coatings are typically structured as metal-dielectric multilayer thin films, which are designed to prevent heat leakage (from the inside of buildings into the environment) by providing strong and very wide-band reflection of thermal infrared wavelengths. Silver-based metal-dielectric multilayer thin-film coatings are very common currently in building windows, which can also offer maximised "light-to-solar gain" – the ratio between the visible light transmittance and solar heat gain coefficient (SHGC).

In recent years, the optical properties of metal-dielectric coatings and their influence on building energy efficiency have been studied extensively due to their superior performance compared to other

multilayer coating structure types. The metal-dielectric coatings performance mainly depends on the choice of materials, and its design philosophy [6-14]. Most (or practically all) products available today from this category (featuring high spectral selectivity and high LSG) employ at least two silver (Ag) layers within their structure, and these coatings cannot withstand prolonged (weeks-scale) exposure to either the ambient atmospheric air or dry-heat test temperatures in excess of 160-180 °C. However, the stability problems of ultrathin Ag layers (normally of less than 20 nm thickness) originate from a range of factors related to the metal layer growth morphology. To overcome these issues, a significant number of research works have been proposed, conducted, and resulted in reporting various solutions, where some of them require more complex materials processing and process parameters optimization [9-18]. Several reports have been published about the properties of various MDC thin-film layer chemistries, including $Ag+SiO_2$, $Ag+TiO_2$, and $Ag+MgF_2$, however, most of them were about metal-dielectric nanoparticle array properties of interest for various applications [19-22]. We previously proposed and partially implemented the development of optimized metal-based RF magnetron co-sputtered MDC (e.g. $Ag+ MgF_2$) layers to replace the pure metal layer in those optical coatings [23, 24]. To the best of our knowledge, the majority of published literature describing Ag-MgF_2 and similar nano-composites research relates to applications other than the product-level development of advanced transparent heat regulating (THR) coatings for use in modern construction. We practically prepared and demonstrated MDC layer-based optical coating building blocks with high structural and optical durability and stability [23, 24], however, until recently we have not explored the color chromaticity properties of those multilayer coating types.

Metal-dielectric thin-film coatings (spectral filters featuring controlled apparent colors) have numerous application possibilities in the fields of building architecture, windows, printed products, and other decorative coatings. There are several reports which have been published in the literature about the color properties of different types of thin-film materials (most of these are single-layer), except a couple of them were found to deal with the color properties of multilayer thin-film structures [25-35]. For example, Dalapati *et. al.*, reported about the preparation and properties of color-tunable low-cost transparent heat reflectors using copper and titanium oxide for energy-saving applications [36]. However, they proposed to control the color properties of the multilayer structures by means of post-deposition annealing process, which can force the metal layer to transform into an array of nanoparticles and can change the optical properties e.g. the transmission spectra. Hence, the color stability of property-optimized application-specific metal-dielectric thin-film coatings and their easy manufacturing process for industrial practices are yet to be achieved for future commercial applications. In this work, we focus on establishing a reliable fabrication process of MDC layers, which can open the new possibilities in engineering and development of new DMD-type coatings with highly durable and reproducible optical and color properties.

2. Growth and characteristics of thin metallic films, metal-dielectric composites, and multilayer structures

We deposited several batches of thin metallic layers, metal-dielectric composites, and multilayer DMD-type building blocks on Corning Eagle XG glass substrates by using the experimentally-determined, fine-tuned process parameters in RF magnetron sputtering systems. In order to achieve very accurate film thickness control for each type of films (either the single layers, or multilayer structures), all the materials/processes used in this work were well calibrated by way of running multiple characterization experiments (described in the Supplementary section). It is very important to have a very precise and controlled growth process for thin metallic films, to enable developing application-specific thin film-based devices and optical components. For example, in DMD-type multilayer structures, thin metallic films play an important role in achieving the required optical transparency, reflectivity and the color of the coatings. It is well known that the deposition of high-quality thin metallic (Ag) layers (of less than 20 nm thickness) requires multi-disciplinary work and research, and involves using technical insights from the fields, such as materials chemistry, nanoscale characterization, and vacuum technology. In the published literature, a claim for the successful fabrication of an ultra-smooth (and ultra-thin, at around 10 nm) Ag layer by using DC magnetron

sputtering system is reported in [37], however, rather than using conventional glass substrates, a specially prepared InP substrate was needed to grow this ultra-thin Ag layer. We made multiple deposition runs to re-confirm the suitability of all the selected process parameters as well as the tooling factor (TF %, a crucial parameter) related to the thin-film growth. Thin Ag layer thickness was monitored during the deposition process with the help of quartz microbalance sensor. Also, from the broad-bandwidth spectral fitting of the measured transmission spectra of Ag (single layer) films with the modelled transmission spectra, the film thicknesses were reconfirmed and then the final tooling factor for the pure metallic targets was recalculated, until stable values were identified. The details of the fine-tuning of this calibration process for thin Ag layer growth are documented in the Supplementary section.

After the successful process development for thin Ag layers, we prepared several batches of metal-dielectric composite (single-layer) films on glass substrates using two separate sputtering targets (Ag and MgF_2), to establish the optimized process parameters to deposit MDC layers. The volumetric content of MgF_2 addition to the pure-metal layer was calculated by using the separately measured partial deposition rates of the sputtering material targets used (calculation details are provided in the Supplementary section). The volumetric content of MgF_2 addition was controlled by the externally applied RF power densities to the both the metallic and dielectric target materials. Figure 1 presents the co-sputtering geometry of the growth of metal-dielectric (Ag/MgF_2) nano-composites.
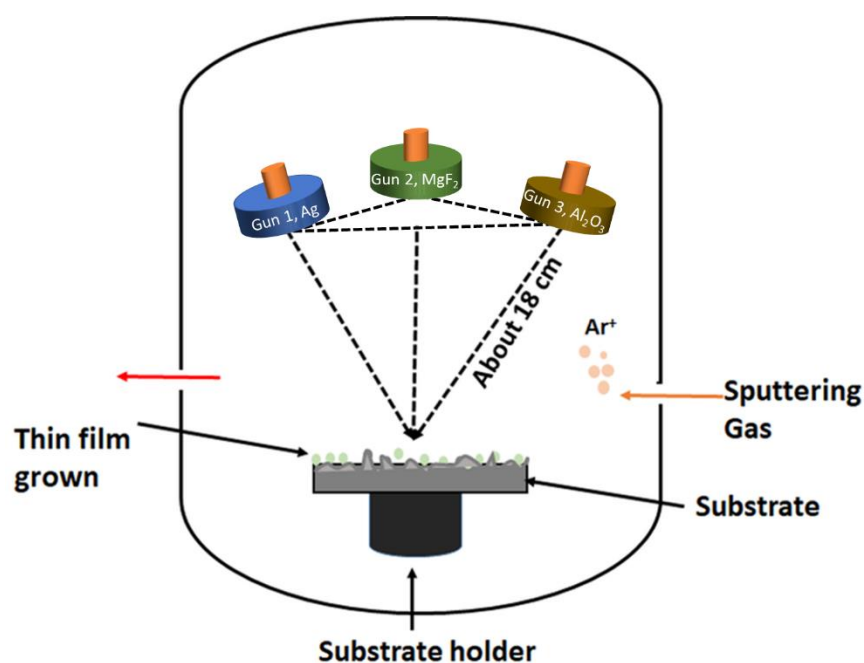

Figure 1. Schematic diagram of the co-sputtering geometry used to prepare the metal-dielectric (Ag/MgF_2) nano-composite thin-film layers.

Later, several batches of DMD-type multilayer coating building blocks using pure silver (Ag) layers, as well as the MDC layers, were fabricated on clear glass substrates. Note that the multilayer structures (D/Ag/D and D/MDC/D types) were deposited in a single deposition run by sequential sputtering of layers using Ag, MgF_2 and ceramic Al_2O_3 sputtering targets with material purity over 99.99%. The process parameters and conditions used to deposit pure Ag, Ag- MgF_2 (single layer) thin-films, and the multilayer structures are summarized in Table 1.

Table 1. Summary of sputtering process parameters and conditions that were used to deposit single-layer thin-films and multilayer coating building blocks.

Process Parameters	Layer Structure (Ag (Single) Layer)	Layer Structure (Metal-dielectric composite (Single) layer)	Layer Structure (DMD type Multilayers)
Sputtering targets (7.62 cm diameter)	Ag	Ag and MgF_2	Ag, MgF_2 and Al_2O_3
Radio frequency (RF) power	64 W	Ag (30 - 64 W), MgF_2 (83 W)	Ag (64 W), MgF_2 (83 W), and Al_2O_3 (199 W)
Base pressure (Torr)	$<3 \times 10^{-6}$–5×10^{-6}	$<3 \times 10^{-6}$–5×10^{-6}	$<3 \times 10^{-6}$–5×10^{-6}
Process gas	Ar	Ar	Ar
Process pressure	2–3 mTorr	2–3 mTorr	2–3 mTorr
Target-to-substrate distance (cm)	~18	~18	~18
Substrate stage rotation rate (rpm)	15–16	15–16	15–16
Substrate temperature (°C)	Room temperature	Room temperature	Room temperature

The optical transmission and color chromaticity properties of single and multilayer films were characterized by using Agilent Cary 5000 spectrophotometer and Konica Minolta 508D colorimeter. The chromaticity values of ultra-thin metallic, MDCs and multilayer structures were characterized based on the Hunter L, a, b color scale. Hunter *L, a, b* color scale is mainly based on the Opponent-Color Theory which assumes that the receptors in the human eye perceive pairs of opposite colors such as light vs. dark, red vs. green, and yellow vs. blue. The L value indicates the level of light or darkness (meaning white or black perceived color) of the sample, while a and b values represent the redness or greenness, and the yellowness or blueness, respectively. Therefore, the explanation of opponent color scale *L, a, b* stands as follows: (i) *L* scale: black vs white; a low number (0-50) indicates the black and a high number (51-100) indicates the white color; (ii) *a* scale: red vs green; a positive number indicates the red color and a negative number indicates the green color; (iii) *b* scale: yellow vs blue; a positive number indicates the yellow color and a negative number indicates the blue color of the sample, as shown in the schematic diagram (Figure 2) [38-42].
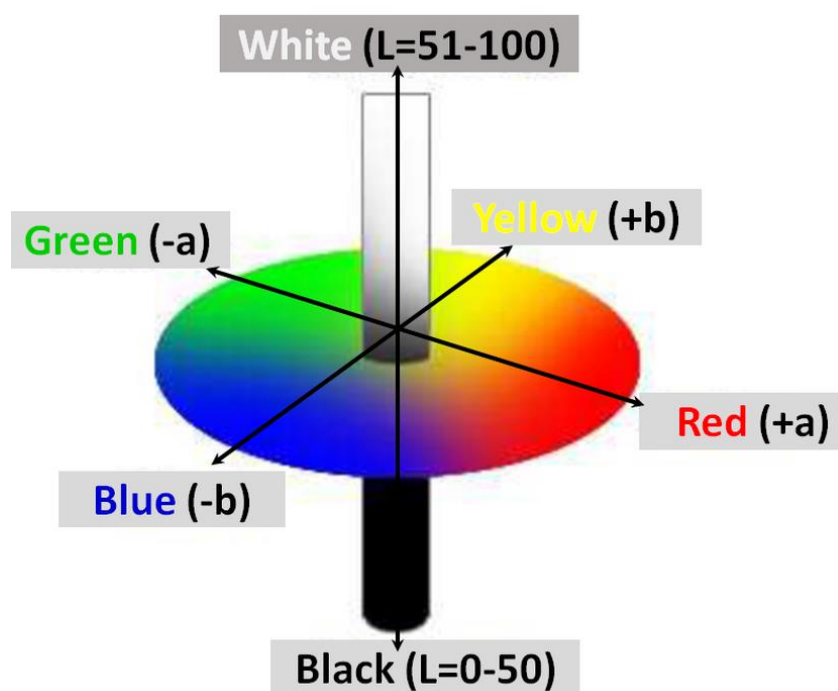

Figure 2. A schematic diagram of the Hunter Lab color space which is also known as the opponent color scale of *L, a, b*.

2.1. Optical and chromaticity properties of single-layer ultrathin metal layers

The spectrally fitted transmission spectra of the as-deposited Ag thin layer with the corresponding modelled transmission spectra (as shown in Figure 3) confirm not only the film thickness but also the successful optimization of thin Ag layer deposition process parameters. More measured transmission spectra (also fitted with the modelled transmission spectra) are provided in the Supplementary section, with the details of optimizing the materials' tooling factors to deposit ultra-thin metallic layers with minimum film thickness errors. Figure 3(a) represents the transmission spectrum of a 17.5 nm as-deposited Ag layer with its modelled (best fitted to 18.2 nm) spectra. From this thickness error, the material's tooling factor was recalculated, and we made multiple deposition runs to finalize the material's tooling factor, as can be confirmed by the very close matching transmission spectra of the ultra-thin 12.6 nm Ag layer, shown in Figure 3(b).
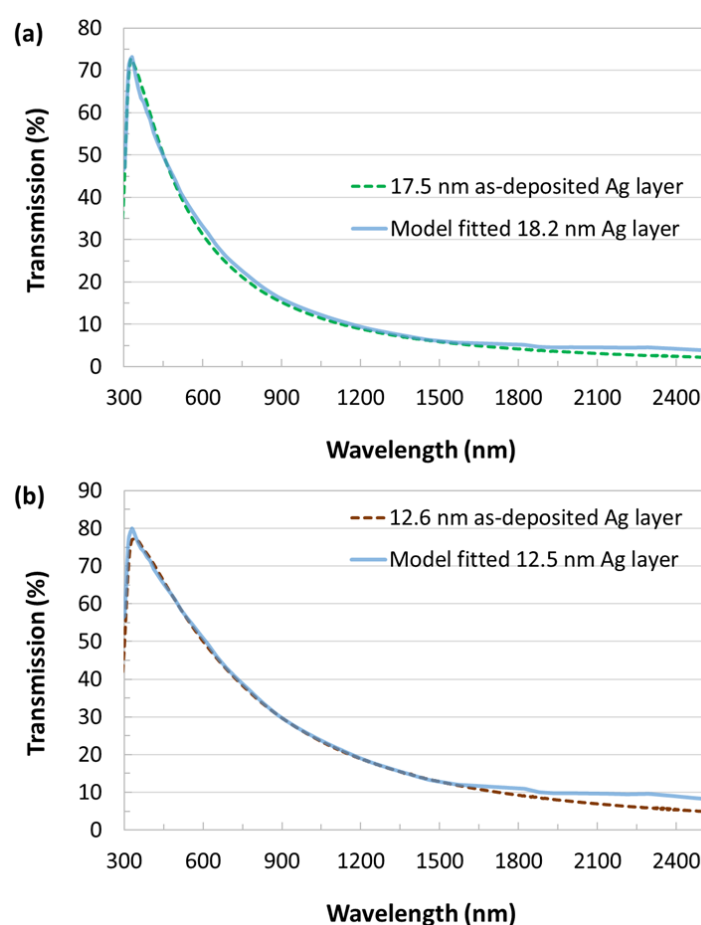

Figure 3. Transmission spectra of thin Ag layers deposited onto clear glass substrates plotted with the best-fitted modelled transmission spectra of corresponding film layers.

The measured Hunter Lab values of as-deposited Ag layers (10-21 nm) are summarized in Table 2. For all single-layer thin Ag films, we focused on the *L* values mostly, rather than *a* and *b* values, as the apparent films' (single layers Ag, or an Ag-dominant nanocomposite) color will mostly be determined by the color (either bright white or transmissive white) that can evaluated by the human eye. The measured *L* values of the as-deposited films were found to be closer to the simulated *L* values (with an accuracy of about 2 %). The reason for having slightly lower *L* values in Ag thin-films, could be due to the thin metallic surface oxidation (films were exposed to room air after the deposition and measurement process, therefore a native oxide could form quickly), however, the measured *a* and *b* values for all Ag samples were found to be positive, in agreement with the simulated values. It can be noticed that the *L* values (both in simulation and measurements) increased with the increasing layer thickness, thus confirming the whitish color of silver layers.

Table 2. Chromaticity characterization results (simulated using OptiLayer Pro software, and measured using Konica Minolta colorimeter, for the light reflected off the coating layers).

Ag layer thickness	Simulated Hunter *L, a, b* (Ra) values			Measured Hunter *L, a, b* (Ra) values		
	L	a	b	L	a	b
10 nm (Model-fitted 9.5 nm)	54.16	4.54	15.37	52.7	2.67	8.62
12.5 nm (Model-fitted 12.6 nm)	66.03	4.57	18.42	64.37	2.58	12
15.6 nm (Model-fitted 15.6 nm)	70.70	4.39	19.17	68.80	2.22	12.26
17.5 nm (Model-fitted 18.2 nm)	75.78	4.08	19.61	74.94	1.68	11.95
21 nm (Model-fitted 22 nm)	81.54	3.69	19.55	80.54	1.05	11.00

The measured optical and chromaticity properties match and fitted well with the simulated values for the single-layer films, confirming the successful deposition and fine control of process parameters used during the deposition of ultrathin Ag layers.

2.2. Optical and chromaticity properties of single-layer ultrathin metal-dielectric composites

Several batches of MDC layers were deposited on glass substrates and the layer thicknesses (during the deposition process) were in-situ controlled by measuring the deposition run time. However, the actual (physical) MDC layer thicknesses were later re-confirmed using the transmission spectrum fitting (comparing the measured and modelled transmission spectra). The transmission spectra of measured MDC layers were fitted (across wide bandwidth) with the modelled nanocomposite layer's transmission spectra, to confirm the actual thickness of the as-deposited MDC layer. Also, the transmission spectra of these MDC layers were fitted and compared with the optically-equivalent (modelled) pure-Ag layers. The modelling of the MDC layers was performed by using a software package (OptiLayer Pro), where the refractive index (n) and extinction coefficient (k) values for the MDC layers were generated by using the weighted-average values of the known dielectric permittivity spectra of both component materials (Ag and MgF_2) .

Figure 4 presents examples of MDC layer physical thickness determination through the optical transmission spectra fittings with the modelled transmission spectra. Figure 4 also shows the calculated absorption coefficients of the MDC layers having different volumetric content of MgF_2 dilution into the metal-dielectric composite matrix. The measured transmission spectra of MDC layers were used to calculate the absorption coefficient spectra of the as-deposited MDC layers by using a simple formula, defined as $T = \exp[-\alpha(\lambda)d]$, where α is the absorption coefficient, T is the transmittance (in percentage), and d is the thickness of the films [43, 44]. The absorption coefficient of the MDC layers were found to be very similar to that of pure-Ag layer. The absorption coefficient of the MDC layers are presented with their calculated upper and lower limits (considering having up to about 5% error in the final film-layer thickness determination). All of the as-deposited MDC layers showed similar trends of the wavelength and film-thickness dependent absorption coefficients. More transmission fitting and absorption coefficient calculation results are provided in the Supplementary section.
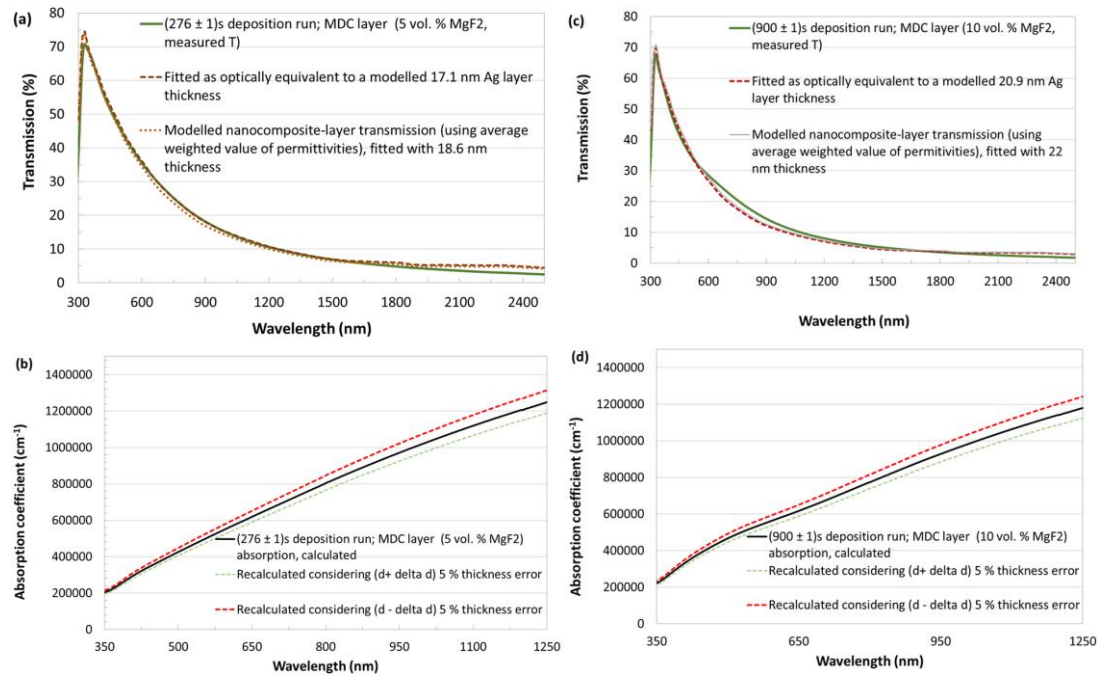
Figure 4. Wavelength-dependent transmission and optical absorption spectra of MDC layer deposited onto clear glass substrates; (a, c) transmission spectrum of thin MDC layer plotted with the best-fitted modelled transmission spectra of spectrally-corresponding film layer and the best-matched optically-equivalent pure-Ag layer; and (b, d) the calculated absorption coefficient spectra of MDC layers considering the estimated max. 5 % thickness errors.

Figure 5 represents the fitted MDC (Ag+ 5 vol. % MgF$_2$) layer thicknesses (brown-colored dot-points) and the thicknesses optically-fitted to the optically-equivalent pure-Ag layers (green-colored diamond-points) data-points, plotted against the "apparent sum" thickness of the nanocomposite layer (as would be determined, in a simplified way, by the simple multiplication of the algebraic sum of the partial deposition rates for Ag and MgF$_2$ and the process duration times). A linear trend of increasing MDC layer thickness, as well as the optically-equivalent Ag layer thickness has been observed with the increasing deposition time. However, the actual MDC layer thicknesses were found to be lower than the simple numerically-calculated "apparent sum" thickness. For example, if Ag was deposited at 5.7 nm per minute and an additional 0.3 nm/min rate applied for the MgF$_2$ deposition for the same process duration, the discrepancy between the "apparent sum" and the actual fitted thickness can then suggest that some degree of inter-solubility, or the "compaction" of materials has been occurring during the nanocomposite formation process. It is also possible that the MgF$_2$ molecules may position themselves in-between the nanoisland- or nanocluster-shaped thin metal volumes, and this could help grow comparatively smoother, dielectric diluted metal-dominant nanocomposite layers. We have noted in our MDC-based Low-E film characterization experiments that an improved correspondence between the spectral design specifications and the measured film spectra were seen frequently, compared to using pure-metal layers; this is the reason we suggest that dielectric dilution could improve interlayer interface quality.

Note that the color chromaticity values (Hunter *L, a, b*) of the MDC layers were also found to be very close to those of optically-fitted equivalent thin Ag layers. The obtained Hunter *L, a, b* values (both measured and simulated) of all the as-deposited MDC layers (Ag+ 5-10 vol. %MgF$_2$) are summarized in Table 3. The measured *L* values for all of the as-deposited MDC layers were found to be close to the simulated *L* values.
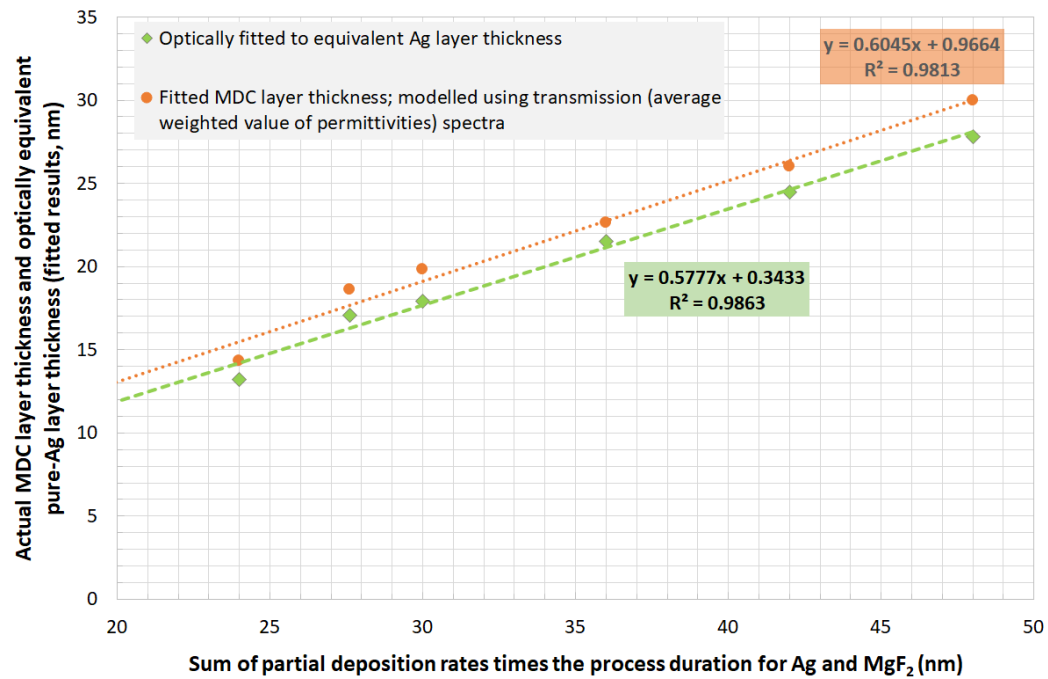
Figure 5. Plot of best-fitted MDC layer thicknesses and the optically-equivalent fitted thicknesses of pure Ag layers.

Table 3. Chromaticity characterization results (Hunter *L, a, b*) of the as-deposited MDC (single) layers.

Sample type		Simulated Hunter L, a, b (Ra) values			Measured Hunter L, a, b (Ra) values		
		L	a	b	L	a	b
As-deposited MDC layers(Ag + 5 vol. % MgF₂)	(240±1)s deposition run (estimated 14.3 nm thick layer)	65.99	4.626	18.52	62.56	1.34	8.37
	(276±1)s deposition run (estimated 18.6 nm thick layer)	74.85	4.18	19.7	70.50	2.17	11.19
	(300±1)s deposition run (estimated 19.8 nm thick layer)	76.86	4.03	19.79	71.04	1.38	9.49
	(360±1)s deposition run (estimated 22.6 nm thick layer)	80.88	3.71	19.74	79.41	1.29	11.16
	(420±1)s deposition run (estimated 26 nm thick layer)	84.73	3.38	19.34	83	0.84	10.34
	(480±1)s deposition run (estimated 30 nm thick layer)	88.13	3.10	18.63	86.67	0.43	9.09
As-deposited MDC layers(Ag + 10 vol. % MgF₂)	(900±1)s deposition run (estimated 22 nm thick layer)	78.5	3.87	19.84	70.80	1.41	8.94

We have noticed that the volumetric fraction of the additional MgF_2 introduced into the composite system had also a significant influence on the color values. An estimated 22 nm MDC layer having 10 vol. % of additional MgF_2 content showed a much lower L values compared to the MDC layer with 5 vol. % (of nearly the same film thickness 22.6 nm), while the a and b values remained almost the same.

2.3. Metal layer based DMD type multilayer structures

DMD-type thin-film multilayers are a widespread and active area of current research in the field of thin-film nanomaterials due to multiple possible applications in optics, photonics, plasmonics, energy generation, and opto-electronics. Despite the relatively extensive history of these studies, especially the silver-based DMD multilayers, these are considered as the prime candidates to be used in heat-mirror applications for many years. This is due to their suitability for adjusting the spectral selectivity (high transmission in the visible spectrum and high reflection in the IR region). We opted to prepare a simple DMD-type structure Al_2O_3 / Ag / Al_2O_3 to use as a reference guide to investigate and compare the features, properties, and the feasibility of the metal-dielectric nanocomposite layers and their integration into the DMD-type multilayer structures. We prepared pure-Ag layer-based trilayer structure (where a 15 nm Ag layer was sandwiched in between two Al_2O_3 layers of the same thickness) using the optimized process parameters for each material system. The multilayer structures were deposited on optically clear glass substrates using a single sequential deposition run in an RF magnetron sputtering system. Figure 6 shows the optical and color chromaticity properties (both measured and simulated) of the trilayer thin-film structures.
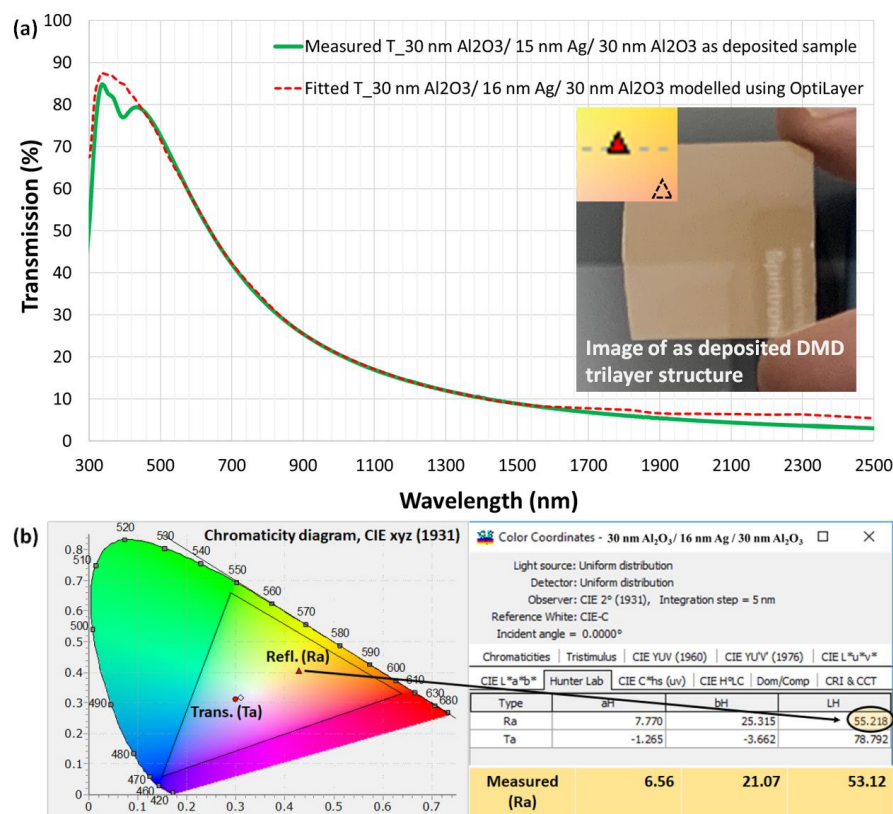

Figure 6. Optical and color chromaticity properties of Al_2O_3 / Ag / Al_2O_3 multilayer building block; (a) measured transmission spectrum plotted with the best-fitted simulated transmission spectrum; the figure legend shows the physical thickness of each particular layer, the inset of the figure shows the simulated color point of film area that matched with the color of the as-deposited trilayer films, (b) shows the Chromaticity diagram (CIE xyz 1931) obtained for the same DMD structure using OptiLayer Pro together with the Hunter *L, a, b* (measured and simulated) values.

The fitted optical transmission spectra of the trilayer structure (shown in Fig. 6a) confirm the successful deposition of DMD type multilayer structure with high accuracy in layer thicknesses. It can be noted that the middle thin metal layer was closely fitted with 16 nm, whilst we deposited 15 nm in the trilayer structure. The measured Hunter *L, a, b* values (Fig. 6b) of the as-deposited trilayer building block were found to be quite close to the simulated values for the same trilayer structure. However, we noticed that the color values of pure Ag layer-based trilayer structures changed (as expected due to high oxidation rate of the pure metal layer) drastically within a couple of days of air exposure in lab conditions (detailed results are presented in Section 2.4). It is important to achieve the structural coatings color with good colorimetric accuracy and durability by way of using repeatable and reliable production methods. Metal-dominant nanocomposites can represent a suitable alternative to replace the pure metal layers in DMD-type multilayer structures and to engineer highly durable application-specific structural coatings with the desired optical and color chromaticity properties. We prepared several batches of MDC-layer based DMD-type multilayer building blocks to investigate the possibility of integration of MDC layers into more complex multilayer coating systems. The optical and color chromaticity properties of MDC-based DMD building blocks are detailed in Section 2.4.

2.4. MDC layer based DMD-type multilayer structures

Al_2O_3 / MDC (Ag + 5 vol. % MgF_2) / Al_2O_3 trilayer building blocks were deposited onto glass substrates where the nanocomposite layer was sandwiched in-between two metal-oxide layers of same type and thickness. Figure 7 shows an example of physical appearance and the optical transmission spectrum obtained from a MDC layer-based trilayer structure. It can be seen that the apparent color of the MDC based structure is quite similar to that of the pure Ag layer based structure (Fig. 7a, b). The obtained transmission spectrum of the MDC-based structures confirms the possibility of engineering and producing new optical coatings, filters or redesigning and modifying the existing coatings by using metal-dominant composite layers, which can then offer better environmental stability properties compared to similar structures based on pure Ag layers. This can be tested and confirmed by running dry-heat exposure tests in air atmosphere; some of the relevant results were previously reported by our group [23, 24, 45]. The measured and simulated color chromaticity (Hunter *L, a, b*) values for several MDC-based D/MDC/D type structures are summarized in Table 4.
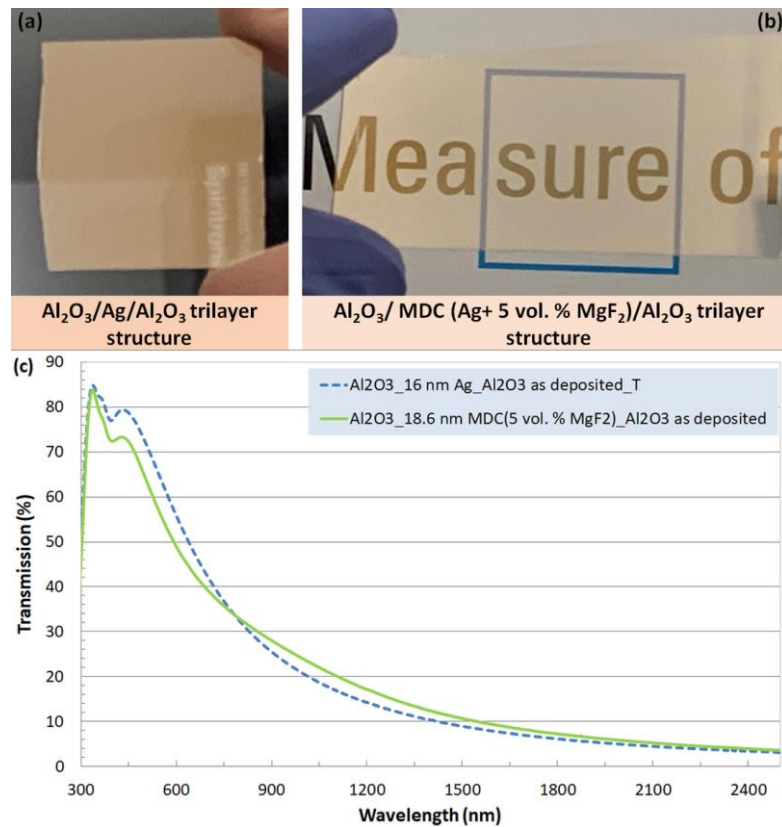
Figure 7. Visual color appearance and optical transmission properties of MDC-based DMD trilayer structure compared to those of pure Ag layer-based DMD trilayer; (a) an image of an as-deposited pure Ag layer based DMD structure, (b) photo of an as-deposited MDC-based trilayer structure, and (c) measured transmission spectra of DMD trilayer structures (pure Ag, and MDC based).

Table 4. Chromaticity characterization results (simulated and measured) for pure Ag layer and MDC layer based trilayer structures.

Sample type	Simulated Hunter L, a, b (Ra) values			Measured Hunter L, a, b (Ra) values		
	L	a	b	L	a	b
30 nm Al_2O_3/ 16 nm Ag/ 30 nm Al_2O_3	55.21	7.77	25.31	53.12	6.56	21.07
30 nm Al_2O_3/ 11.8 nm MDC/ 30 nm Al_2O_3	39.64	8.58	19.12	39.28	6.40	15.03
30 nm Al_2O_3/ 18.6 nm MDC/ 30 nm Al_2O_3	59.85	7.29	26.52	55.80	4.8	20.29
30 nm Al_2O_3/ 19.8 MDC/ 30 nm Al_2O_3	62.77	6.86	27.09	60.43	4.85	21.86

From the obtained results, it can be concluded that it is possible to fabricate multilayer structures using even a relatively thicker MDC layer without compromising much of the optical

and chromaticity properties (as confirmed by the optical transmission spectra of Fig. 7c and the L values for the structures 30 nm Al_2O_3/ 16 nm Ag/ 30 nm Al_2O_3 and 30 nm Al_2O_3/ 18.6 nm MDC/ 30 nm Al_2O_3). Figure 8 (a) shows the measured optical transmission spectra of several MDC-based as-deposited trilayers where the MDC layer thickness varied from 13.6 nm to 30 nm. The obtained spectral shapes show that the thicker the middle MDC layer, the higher is the IR reflection and also the higher the values of L. Higher L values confirms the increased brightness (visual apparent color of the coatings being closer to white). We have experimentally tested the color stability of the MDC based coatings compared to the coatings based on pure Ag. We have selected two structures (30 nm Al_2O_3/ 16 nm Ag/ 30 nm Al_2O_3, and 30 nm Al_2O_3/ 18.6 nm MDC/ 30 nm Al_2O_3) to investigate the stability of the color values by way of measuring the color values on different days, during a lab storage test. The color stability test results obtained are presented in Figure 8(b). It can be seen that the L value of the pure Ag layer-based structure has changed drastically within the first seven days after the deposition, while the MDC-based coating structure showed a minimal change in the measured L values. We have also noted that the Hunter a and b values in both trilayer types did not show significant changes on the same time-scale.
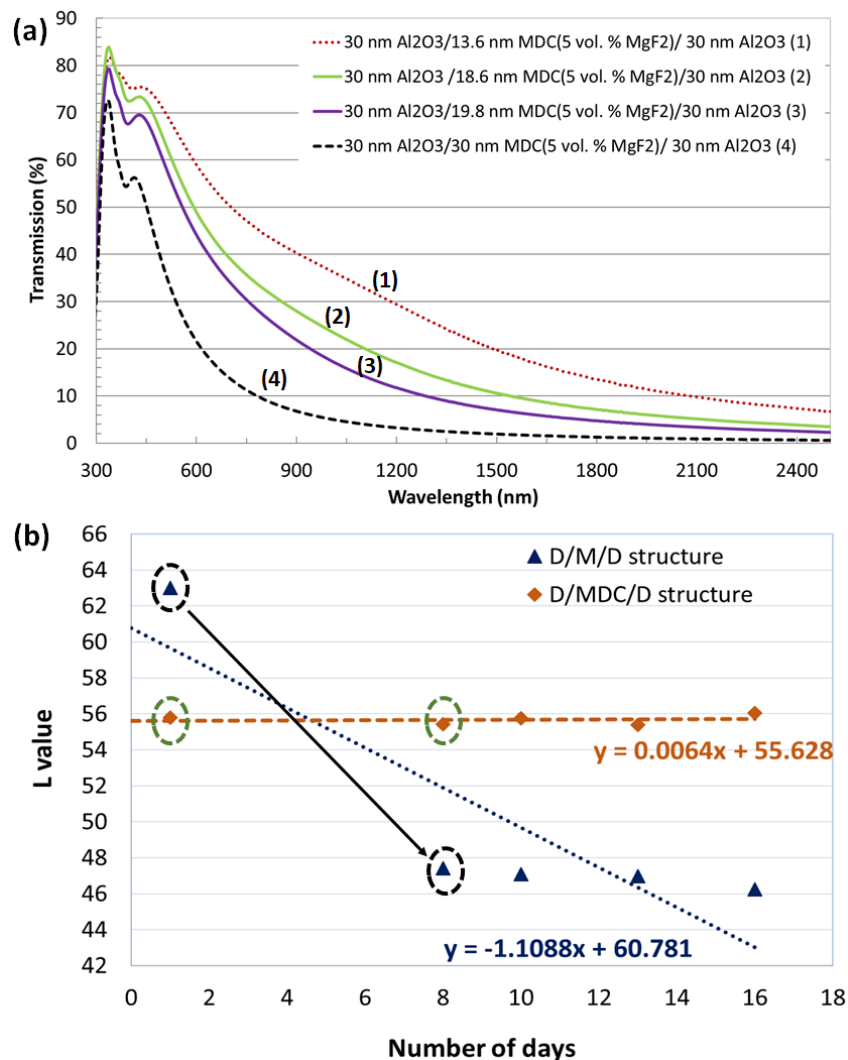

Figure 8. Optical and color chromaticity properties of MDC-based trilayer structures; (a) measured transmission spectra of trilayer structures prepared with different MDC layer thickness, and (b) Hunter L value stability investigation results based on air atmosphere exposure time.

The changes in L values (negative trend) observed in the pure metal-based trilayer structure suggests that the Ag layer degradation (due to possible silver oxidation) occurred within the DMD

structure, and this likely changed the overall film color properties, which manifested in the observed *L* value changes. On the other hand, the MDC based coating structure showed an almost unchanged *L* value (a slightly positive change in *L* has been noted) during up to 15 days of testing.

3. Summary

The design variations, material inter-compatibility issues, and the optical and chromaticity properties of the MDC-based coatings have been investigated and compared to those of pure metallic layer-based trilayer building blocks of low-emissivity coatings. The study has focused on the optical performance and environmental stability characteristics of silver-containing thin and ultrathin coating structures. Magnesium fluoride-containing MDC layers can be used to enable arbitrarily complex high-stability low-E, heat-mirror, or spectral filter-type optical coating designs of high spectral selectivity, on a range of optical substrates. In terms of color stability, it has been confirmed that the MDC layers can provide more design flexibility in structural optical coatings with the potentially improved tuneability of the apparent color essential for various modern industrial and commercial applications.

The co-deposited metal-dielectric nanocomposites (MDC), in which the volumetric content of the dielectric phase were within 5-10 vol. % are semi-metallic substances (often termed cermets in the literature) of solid solution type that can represent an alternative coating design option, compared to using pure metallic layers. The development of MDCs of composition type $Ag:MgF_2$ was expected to accomplish the following: (i) promote adhesion of the metallic layers to their substrates, (ii) promote mechanical hardness of soft plasmonic metal layers, (iii) improve metal layer morphology by way of "filling the pores" between ultrathin metal nano-islands, and (iv) potentially smoothen the interface roughness in ultrathin metallic layers. The preliminary experimental results obtained in this work confirmed that these types of nanocomposite type metal-rich materials will enable the design and fabrication of advanced new types of multilayer optical coatings, even though a number of further studies of these nanocomposite materials are still required. Additionally, it is possible to engineer a broader range of reflected or transmitted color properties, compared to pure metal-based designs.

4. Conclusions

We have established the RF sputtering deposition process of metal-dielectric composite layers and developed MDC layer-based trilayer structures of interest for use as building blocks in future low-emissivity coatings. The possibility of engineering multilayer optical coatings with improved stability of the transmission spectrum and apparent color properties has been experimentally demonstrated. Dielectric/MDC/Dielectric type trilayer structures provide new options in the design and engineering of next-generation optical coatings enabling new applications in building energy efficiency, architectural glass coatings, heat-shields, and decorative coating products.

References

1. Chu, S.; Majumdar, A. Opportunities and challenges for a sustainable energy future. *Nature,* **2012**, *488*, 294.
2. International Energy Outlook 2010, a report by the Office of Integrated Analysis and Forecasting, U.S. Energy Information Administration, U.S. Department of Energy (July 2010), available from http://www.eia.doe.gov/oiaf/ieo/pdf/0484(2010).pdf.
3. H. J. Gläser, Large Area Glass Coating (Von Ardenne Anlagentechnik GmbH, Dresden, Germany, 2000).
4. Dalapati, G.K.; Kushwaha, A.K.; Sharma, M.; Suresh, V.; Shannigrahi, S.; Zhuk, S.; Masudy-Panah, S. Transparent heat regulating (THR) materials and coatings for energy saving window applications: Impact of materials design, micro-structural, and interface quality on the THR performance. *Progress in materials science* **2018**, *95*, 42-131.
5. Vasiliev, M.; Nur-E-Alam, M.; Alameh, K. Recent developments in solar energy-harvesting technologies for building integration and distributed energy generation. *Energies*, **2019**, *12(6)*,1080.
6. Peres, L.; Bou, A.; Barakel, D.; Torchio, P. ZnS/ Ag/ TiO$_2$ multilayer electrodes with broadband transparency for thin film solar cells. *RSC Advances* **2016**, *6*, 61057-61063.
7. Kim, J.-H.; Kim, D.-H.; Kim, S.-K.; Bae, D.; Yoo, Y.-Z.; Seong, T.-Y. Control of refractive index by annealing to achieve high figure of merit for TiO2/Ag/TiO2 multilayer films. *Ceramics International* **2016**, *42*, 14071-14076.
8. Pracchia, J.; Simon, J. Transparent heat mirrors: influence of the materials on the optical characteristics. *Applied optics* **1981**, *20*, 251-258.
9. Leftheriotis, G.; Yianoulis, P.; Patrikios, D. Deposition and optical properties of optimised ZnS/Ag/ZnS thin films for energy saving applications. *Thin solid films* **1997**, *306*, 92-99.
10. Kulczyk-Malecka, J.; Kelly, P.; West, G.; Clarke, G.; Ridealgh, J.; Almtoft, K.; Greer, A.; Barber, Z. Investigation of silver diffusion in TiO2/Ag/TiO2 coatings. *Acta Materialia* **2014**, *66*, 396-404.
11. Wang, Z.; Cai, X.; Chen, Q.; Chu, P.K. Effects of Ti transition layer on stability of silver/titanium dioxide multilayered structure. *Thin Solid Films* **2007**, *515*, 3146-3150.
12. Wang, L.; Shen, Z.; Du, G.; Wang, P.; Wang, P. The thermal stability of silver-based high reflectance coatings. *Thin Solid Films* **2016**, *616*, 122-125.
13. Mosquera, A.A.; Albella, J.M.; Navarro, V.; Bhattacharyya, D.; Endrino, J.L. Effect of silver on the phase transition and wettability of titanium oxide films. *Scientific reports* **2016**, *6*, 32171.
14. Mohelnikova, J. Materials for reflective coatings of window glass applications. *Construction and Building Materials* **2009**, *23*, 1993-1998.
15. Carton, O.; Ghaymouni, J.; Lejeune, M.; Zeinert, A. Optical characterization of porous sputtered silver thin films. *Journal of Spectroscopy*, **2013**, *1*, 307824.
16. Chen, W.; Thoreson, M. D.; Kildishev, A. V.; Shalaev, V. M. Ultra-thin ultra-smooth and low-loss silver and silver-silica composite films for superlensing applications, CLEO: QELS_Fundamental Science, San Jose, California, United. States. https://engineering.purdue.edu/~shalaev/Publication_list_files/QThE4.pdf 2010.
17. Anders, A.; Byon, E.; Kim, D.; Fukuda, K.; Lim, S. N. Smoothing of ultrathin silver films by transition metal seeding. *Solid State Commun*., **2006**, *140(5)*, 225–229.
18. Bulir, J.; Novotny, M.; Lynnykova, A.; Lancok, J. Preparation of nanostructured ultrathin silver layer. *J. Nanophotonics*, **2011**, *5(1)* 051511.
19. Jiang, X.; Chen, S.; Mao, C. Synthesis of Ag/SiO2 nanocomposite material by adsorption phase nanoreactor technique. Colloids and Surfaces A: Physicochemical Engineering Aspects, **2008**, *320*, 104–110.
20. Yu, B.; Leung, K. M.; Guo, Q.; Lau W. M.; Yang, J. Synthesis of Ag–TiO$_2$ composite nano thin film for antimicrobial application. *Nanotechnology*, **2011**, *22*, 115603.
21. Cummings, K. D.; Garland, J. C.; Tanner, D. B. Optical properties of a small-particle composite. *Physical Review B*, **1984**, *30 (8)*, 4170-4182.
22. Zhao, Y. L.; Xu, X.; Ming, H. Ag-MgF$_2$ composite films deposited by RF magnetron sputtering. *J. Functional Materials*, **2007**, 38(3), 386-388.
23. Nur-E-Alam, M.; Lonsdale, W.; Vasiliev, M.; Alameh, K. Application specific oxide-based and metal-dielectric thin-film materials prepared by radio frequency magnetron sputtering. *Materials*, **2019**, 12 (20) 3448.

24.   Dalapati, D.K.; Sharma, M. Energy Saving Coating Materials, Ch.4, in press, Elsevier and Thomson Digital, **2020.**

25.   Chen, L.; Chen, N.; Li, Y.; Li, W.; Zhou, X.; Wang, Z.; Zhao, Y.; Bu, Y. Metal-dielectric pure red to gold special effect coatings for security and decorative applications. _Surface and Coatings Technology_ **2019**, _363_, 18-24.

26.   Schueler, A.; Roecker, C.; Scartezzini, J.-L.; Boudaden, J.; Videnovic, I.; Ho, R.-C.; Oelhafen, P. On the feasibility of colored glazed thermal solar collectors based on thin film interference filters. _Solar Energy Materials and Solar Cells_ **2004**, _84_, 241-254.

27.   Orel, B.; Spreizer, H.; Vuk, A.Š.; Fir, M.; Merlini, D.; Vodlan, M.; Köhl, M. Selective paint coatings for coloured solar absorbers: Polyurethane thickness insensitive spectrally selective (TISS) paints (Part II). _Solar Energy Materials and Solar Cells_ **2007**, _91_, 108-119.

28.   Bu, Y.; Guo, R.; Li, Y.; Meng, Z.; Chen, N. All-dielectric metameric filters for optically variable devices. _Chinese Optics Letters_ **2014**, _12_.

29.   Kalfagiannis, N.; Logothetidis, S. Color dependency on optical and electrical properties of TiN_x thin films. _Rev. Adv. Mater. Sci._ **2007**, 15, 167-172.

30.   Rashid, H. G.; Mishjil, K. A.; Habubi, N. F. Color space chromaticity diagram: Estimation of Co impurity ratios in SnO_2 thin films

31.   Ellenbogen, T.; Seo, K.; Crozier, K. B. Chromatic plasmonic polarizers for active visible color filtering and polarimetry. _Nano Lett._, **2012**, 12, 1026-1031.

32.   Diest K.; Dionne, J. A.; Spain, M.; Atwater, H. A. Tunable color filters based on metal-insulator-metal resonators. _Nano Lett._, **2009**, 9(9), 2579-2583.

33.   Xu, T.; Shi, H.; Wu, Y. K.; Kaplan, A. F.; Ok, J. G.; Guo, L. J. Structural colors: From plasmonic to carbon nanostructures. _Small_, **2011**, 7(22), 3128-3136.

34.   Song, M.; Wang, D.; Peana, S.; Choudhury, S.; Nyga, P.; Kudyshev, Z. A.; Yu, H.; Boltasseva, A.; Shalaev, V. M.; Kildishev, A. V. Colors with plasmonic nanostructures: A full-spectrum review. _Appl. Phys. Rev._, **2019**, 6, 041308.

35.   Song, H. S.; Lee, G. J.; Yoo, D. E.; Kim, Y. J.; Yoo, Y. J.; Lee, D. W.; Siva, V.; Kang, I. S.; Song, Y. M. Reflective color filter with precise control of the color coordinate achieved by stacking silicon nanowire arrays onto ultrathin optical coatings. _Sci. Rep._, 2019, 9, 93350.

36.   Dalapati, G.K.; Masudy-Panah, S.; Chua, S.T.; Sharma, M.; Wong, T.I.; Tan, H.R.; Chi, D. Color tunable low cost transparent heat reflector using copper and titanium oxide for energy saving application. _Scientific reports_ **2016**, _6_, 20182.

37.   Devaraj, V.; Lee, J.; Baek, J.; Lee, D. Fabrication of ultra-smooth 10 nm silver films without wetting layer. _Appl. Sci. Converg. Technol_. **2016**, 25(2), 32-35.

38.   Robartson, A. R. The CIE 1976 color-difference formulae. _Color Res._, **197**7, 2, 7-11.

39.   https://support.hunterlab.com › en-us › article_attachments (Accessed on 10/01/2020).

40.   Lovetskiy, K. P.; Sevastianov, L. A.; Nikolaev, N. E. Numerical modeling of color perception of optical radiation. _Mathematical Modelling and Geometry_. **2018**, 6 (1), 21 – 36.

41.   https://www.pce-italia.it/html/dati-tecnici-1/misuratore-di-colore-cta.htm (Accessed on 12/01/2020).

42.   https://www.pce-instruments.com/turkish/oel_uem-teknolojisi/oel_uem-cihazlarae_/spektrometre-spektrofotometre-kat_159226.htm (Accessed on 13/01/2020).

43.   Abass, K. H. Fe_2O_3 thin films prepared by spray pyrolysis technique and study the annealing on its optical properties. _International letters of Chemistry, Physics and Astronomy_. **2015**, 45, 24-31.

44.   Cho, S. Optical and electrical properties of CuO thin films deposited at several growth temperatures by reactive RF magnetron sputtering. _Met. Mater. Int_., **2013**, 19(6), 1327-1331.

45.   Vasiliev, M.; Nur-E-Alam, M.; Alameh, K. Highly stable thin-film multilayers for thermal regulation and energy savings in smart cities. 16th IEEE International Conference on. Smart Cities: Improving Quality of Life. Using ICT, IoT & AI. UNC Charlotte, NC, USA. October 06-09, 2019.